

Ophthalmic Artery Morphological and Hemodynamic Features in Acute Coronary Syndrome

Lan-ting Wu, Jia-lin Wang, and Yan-ling Wang

Department of Ophthalmology, Beijing Friendship Hospital, Capital Medical University, Beijing, China

Correspondence: Jia-lin Wang,
Department of Ophthalmology,
Beijing Friendship Hospital, Capital
Medical University, Beijing 100050,
China;

wangjialin@bjmu.edu.cn.

Yan-ling Wang, Department of
Ophthalmology, Beijing Friendship
Hospital, Capital Medical University,
Beijing 100050, China;
wangyanl@ccmu.edu.cn.

JW and YW contributed equally to
the work presented here and should
therefore be regarded as equivalent
authors.

Received: June 1, 2021

Accepted: October 18, 2021

Published: November 10, 2021

Citation: Wu LT, Wang JL, Wang YL.
Ophthalmic artery morphological
and hemodynamic features in acute
coronary syndrome. *Invest
Ophthalmol Vis Sci.* 2021;62(14):7.
<https://doi.org/10.1167/iovs.62.14.7>

PURPOSE. To examine the morphological and hemodynamic changes of the ophthalmic artery (OA) in patients with acute coronary syndrome (ACS).

METHODS. This cross-sectional observational study included 31 patients with ACS and 10 healthy controls (HCs). The ACS subgroups were ST-segment elevation myocardial infarction (STEMI; $n = 10$), non-STEMI ($n = 10$), and unstable angina ($n = 11$). OA three-dimensional (3D) models were reconstructed based on computed tomographic angiography, and morphological aspects of the OA were measured quantitatively. Moreover, numerical simulation by computational fluid dynamics was used to obtain hemodynamic information of the OA.

RESULTS. The study reconstructed 41 OA models. Hemodynamic simulation revealed a significant decrease in OA blood velocity in patients with ACS compared with the HCs (median velocity, 0.046 vs. 0.147 m/s; $P < 0.001$). No differences in the morphological data for the OA were observed. Also, no differences in the mass flow ratio of OA to the ipsilateral internal carotid artery was found. Similar differences were observed between the ACS subgroups and HCs. OA blood velocity was negatively correlated with body mass index, abdominal circumference, left ventricular ejection fraction, and triacylglycerol and was positively correlated with early to late transmitral flow velocity, N-terminal pro-brain natriuretic peptide, serum creatinine, and potassium.

CONCLUSIONS. The initial OA blood velocity was slower in patients with ACS and was associated with ACS-related clinical parameters. To our knowledge, this is the first study to analyze OA characteristics in ACS using 3D model reconstruction and hemodynamic simulation, providing new perspectives on the relationship between ischemic heart disease and ocular manifestations.

Keywords: ophthalmic artery, acute coronary syndrome, three-dimensional reconstruction, computational fluid dynamics, blood velocity

Acute coronary syndrome (ACS), which is the acute manifestation of ischemic heart disease, remains a leading cause of morbidity and mortality worldwide.¹ Several studies have been conducted on the pathology and prognosis of ischemic heart disease from the perspective of the ocular vessels. Notably, the ocular vessels may be a guiding factor for the long-term prognosis of patients with ACS. Wang et al.² reported that the degree of retinal atherosclerosis was closely related to the recurrence of ACS. Furthermore, cases of retinal artery occlusion after percutaneous coronary intervention (PCI) have been reported worldwide.³ In contrast, ocular vascular disease may also harbor ACS. Studies have reported that patients with retinal vascular occlusion had a higher risk of ACS.⁴⁻⁶

Accordingly, it is vital to understand the relationship between ischemic heart disease and ocular blood flow. Many studies have explored retinal vascular parameters in ACS, such as superficial retinal capillary plexus vascular density, but the results remain controversial.⁷⁻¹⁰ Most have focused on the variables of retinal blood flow. Nevertheless, the blood supply of the eye originates from the ophthalmic

artery (OA), which is believed to be a more direct and accurate response to ocular blood flow.

The OA is difficult to observe clinically due to its small diameter and complex course. Digital subtraction angiography (DSA) and color Doppler imaging (CDI) are widely used to visualize the OA; however, DSA is invasive, and patients may present with varying degrees of complications. When applied to the retrobulbar vessels, CDI results may be influenced by human factors and therefore may be of limited use in visualization of the OA. Computed tomographic angiography (CTA) has been increasingly applied in neurovascular imaging. A greater number of slice images yields a clearer display of the complex vascular trees and their adjacent structures. We adapted computer software to reconstruct three-dimensional (3D) OA models based on CTA images and obtained anatomical information regarding the initial OA, the junction of the OA and internal carotid artery (ICA). In terms of hemodynamic simulation, computational fluid dynamics (CFD) has recently attracted clinical interest. Numerical simulation based on CFD can be used to obtain accurate hemodynamic information of diseased vessels in

patients. The models are consistent with the shape of vessels under clinical conditions. Thus, the flow-field analysis results according to the simulation are convincing. This approach has been used for the hemodynamic analysis of, for example, aortic aneurysms, carotid artery stenosis, and stented coronary arteries.^{11–13} However, it has not been applied to retrolubar vessels.

Our study aimed to investigate the changes in the morphology and hemodynamics of the OA in patients with ACS and to explore whether the characteristics of the OA were related to the clinical parameters of ACS.

METHODS

Study Design and Data Collection

This was a cross-sectional observational study of the difference between the morphology and hemodynamics of the OA in patients with ACS and healthy controls (HCs). The study protocol was approved by the local ethics committee of Beijing Friendship Hospital (2020-P2-008-01) and was conducted in accordance with the tenets of the Declaration of Helsinki, the International Conference on Harmonization Good Clinical Practice guidelines, and applicable Chinese laws. All participants provided written informed consent.

The medical records of all patients with ACS admitted to the Beijing Friendship Hospital from January 2020 to September 2020 who underwent CTA and those of healthy individuals who underwent CTA for other reasons were reviewed. All patients with ACS had a clear diagnosis and thus underwent coronary angiography. The hospital electronic medical records were verified, and parameters were collected and recorded. Each participant then underwent a detailed ocular examination, including Snellen best-corrected visual acuity, intraocular pressure (by non-contact tonometry), slit-lamp examination, fundus color photography, axial length measurement by optical biometry (IOL Master; Carl Zeiss Meditec, Jena, Germany), and optical coherence tomography (OCT; Heidelberg Engineering, Heidelberg, Germany). The exclusion criteria were as follows: (1) any existing eye refractive medium opacity, orbital space-occupying diseases, glaucoma, optic neuritis glaucoma, or other significant eye pathologies such as blindness and inability to fixate; (2) intracranial space-occupying lesions and fundus lesions caused by systemic diseases, such as diabetes and high blood pressure; and (3) active syphilis, hepatitis B, or other infectious diseases.

CTA Acquisition

CTA was performed using a 64-row multidetector CT scanner (LightSpeed VCT; GE Healthcare, Chicago, IL, USA) extending from the arch of the aorta to the skull base. An injection of 65 mL of contrast medium (iohexol, 300 mg iodine per mL) through an 18-gauge needle using a power syringe at a rate of 4 mL/s was administered into the antecubital vein. A smart prep layer was set to scan the starting position. The starting scanning threshold was set at 140 Hounsfield units, and it started when the CT value reached the threshold scan. The scanning parameters were as follows: pixel spacing, 0.625 mm; image resolution, 512 × 512; layer spacing, 0.8 mm; machine rack rotation speed, 39.37 mm/rotation; rack rotation time, 0.5 s/rotation; and pitch, 0.984. The raw data of the CTA images were stored in a DICOM format.

3D OA Reconstruction

DICOM images were imported into Mimics 21.0 (Materialise, Ann Arbor, MI, USA) for reconstruction. We reconstructed one of the OAs that was visible on the CTA for each subject. Image segmentation technology was performed to extract clear contour data of the OA and ICA from CT images; Figure 1A shows the origin of the OA on the CTA images. The specific process is as follows: (1) Determine the region of the target tissue structure to be segmented in the tomography image. Use the threshold segmentation function to create a new mask. Based on our experience, slightly adjust the threshold of this mask with reference to the OA so that the pixels of this mask fill the OA as much as possible. (2) Edit the mask of the above objects based on their 3D form, erase other interfering objects, and only retain a certain length of common carotid artery, external carotid artery, ICA, and OA. The region growing function was used to grow and select the ICA and OA region so as to obtain a new mask with all pixel points continuous and to separate the other part connected with the ICA and OA. (3) Use the calculate 3D function to perform the optimal quality operation on the above mask to obtain a 3D model of the OA containing the above pixel points. After reconstruction, models were imported into Geomagic Studio 14.0 (3D Systems, Rock Hill, SC, USA) to smooth the model surface and form solid blood vessel models (Fig. 1B).

The centerline best-fit diameter of the initial OA was measured, as was the angle between the OA and ICA centerlines (Fig. 1C). All of the above results were evaluated and analyzed by two experienced ophthalmologists.

CFD Simulation

A finite-volume method for steady flow was used in the simulation calculation using Ansys Fluent 15.0 (Ansys, Inc., Canonsburg, PA, USA). Each model was discretized into approximately 0.3 million tetrahedron and tri-prism mixed elements using Ansys ICEM CFD. A simple algorithm for the calculation of blood velocity and pressure base was selected to correct the pressure and solve the momentum equation in sequence. The vessel wall was considered rigid and no slip, and the simulated blood was assumed to be a steady-state, laminar, and incompressible Newtonian fluid. The Navier—Stokes equation and mass conservation equation are governing equations for the numerical simulation:

$$\rho (\vec{u} \cdot \nabla) \vec{u} + \nabla p - \mu \Delta \vec{u} = 0 \quad (1)$$

$$\nabla \cdot \vec{u} = 0 \quad (2)$$

In the formula, ρ represents the blood density, \vec{u} represents the velocity vector, p represents the pressure, and μ represents the blood viscosity. Then, the material attribute values of blood were set ($\mu = 3.5 \times 10^{-3}$ kg/ms; $\rho = 1050$ kg/m³). We adopted the averaged systolic and diastolic blood flow velocity of 0.34 m/s¹⁴ as the inlet velocity (the flow rate into the siphon of the ICA). A pressure boundary condition of 0 Pa was set at the outlet. All models adopted the same boundary conditions and parameters.

After the calculation, the fluid velocity streamline chart was created using the post-processing software in Ansys

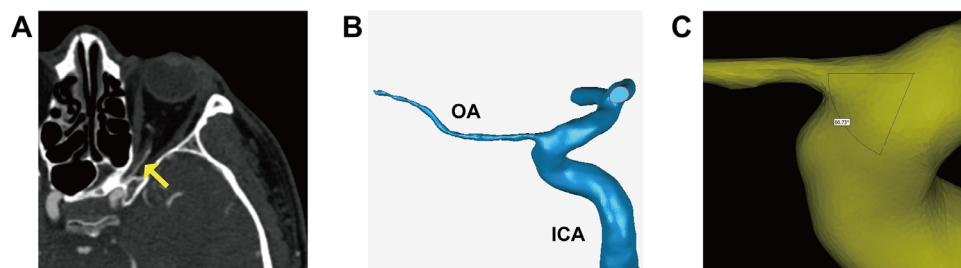


FIGURE 1. Case example of a 3D OA model reconstructed from the CTA images. (A) The beginning of the OA can be seen on the CTA image (yellow arrow). (B) The 3D model after being smoothed using Geomagic Studio 14.0. (C) Measurement of the angle between the OA and ICA using Mimics.

Fluent. The mass flow was calculated using Flux Reports, and the fraction of the ICA flowing into the OA was calculated.

Statistical Analysis

Continuous variables were tested for normality using the Shapiro–Wilk test. Descriptive data with a normal distribution are expressed as the mean \pm SD, and those with non-normal distribution are expressed as median (25th–75th percentile); comparisons were made using the *t*-test or Mann–Whitney *U* test. When multiple groups were compared, one-way ANOVA was used for normally distributed continuous variables, whereas the Kruskal–Wallis *H* test was used for non-normally distributed variables. Categorical variables are presented as numbers and percentages and were analyzed using the χ^2 test or Fisher's exact test, as appropriate. Bonferroni correction was used for multiple comparisons.

Pearson's correlations and linear regression were used to estimate linear relationships between continuous variables. Continuous variables that were not normally distributed were transformed into natural logarithms. Statistical analyses were carried out using SPSS Statistics 26.0 (IBM, Chicago, IL, USA). $P \leq 0.05$ was considered statistically significant.

RESULTS

Baseline Characteristics

Thirty-one patients with ACS (mean age, 62.48 ± 4.69 years; 26% female) and 10 healthy controls (mean age, 59.40 ± 8.30 years; 40% female) were included in the study. The clinical characteristics of the patients are summarized in Table 1. Patients with ACS had a higher rate of comorbidities, including hypertension, dyslipidemia, and diabetes

mellitus, compared with HC. No differences were found for age, sex, current smoking status, or history of ischemic stroke in patients with ACS compared with the HCs.

Clinical characteristics, laboratory parameters, cardiac hemodynamic variables, and concomitant medication of the ACS subgroups are shown in Table 2. Subgroups of ACS included patients with an ST-segment elevation myocardial infarction (STEMI; $n = 10$), non-STEMI (NSTEMI; $n = 10$), and unstable angina (UA; $n = 11$). Except for three participants in the UA group, all other participants underwent PCI or coronary artery bypass graft (CABG) before the CTA examination. To avoid impacting the ICA, we evaluated the degree of ICA stenosis in all participants through CTA imaging. Based on the North American Symptomatic Carotid Endarterectomy Trial,¹⁵ one patient had mild ICA stenosis, two patients had moderate stenosis, and two patients had severe stenosis in both the STEMI and UA groups. In the NSTEMI group, only one patient had mild stenosis and one patient had severe stenosis. Mean axial length was 23.90 ± 0.91 mm in the HCs, 24.27 ± 1.15 mm in the STEMI group, 24.22 ± 1.16 mm in the NSTEMI group, and 24.26 ± 1.00 mm in the UA group. There was no statistically significant difference between each group ($P = 0.837$). Also, OCT showed no obvious abnormalities in any participant.

Morphological Comparison

CTA was available for all participants, and the OAs from 41 patients were reconstructed. Quantitative measurements demonstrated that the mean diameter of the initial OA in HCs was 1.56 ± 0.37 mm. The median (25th–75th percentile) angle between the OA and ICA was 76.72° (70.81° – 81.33°). No difference was found in the OA diameter or angle ($P = 0.840$, $P = 0.976$, respectively).

TABLE 1. Baseline Characteristics of the Participants

Variables	Group		<i>P</i>
	HC ($n = 10$)	ACS ($n = 31$)	
Age (y), mean \pm SD	59.40 ± 8.30	62.48 ± 4.69	0.287
Female sex, n (%)	4 (40)	8 (26)	0.391
Current smoking, n (%)	3 (30)	20 (65)	0.075
Hypertension, n (%)	5 (50)	27 (87)	0.014*
Dyslipidemia, n (%)	4 (40)	27 (87)	0.003**
Diabetes mellitus, n (%)	1 (10)	22 (71)	<0.001***
History of ischemic stroke, n (%)	1 (10)	13 (42)	0.064

$P < 0.05$ is significant (bold values). * $P < 0.05$; ** $P < 0.01$; *** $P < 0.001$.

TABLE 2. Baseline Characteristics of ACS Subgroups

Variables	STEMI (n = 10)	NSTEMI (n = 10)	UA (n = 11)
Clinical characteristics			
Age (y), mean ± SD	62.20 ± 6.16	63.10 ± 4.10	62.18 ± 4.02
Female sex, n (%)	1 (10)	3 (30)	4 (36)
Current smoking, n (%)	8 (80)	5 (50)	7 (64)
Hypertension, n (%)	6 (60)	10 (100)	11 (100)
Dyslipidemia, n (%)	8 (80)	8 (80)	11 (100)
Diabetes mellitus, n (%)	6 (60)	8 (80)	8 (73)
PAD, n (%)	1 (10)	3 (30)	4 (36)
History of ischemic stroke, n (%)	4 (40)	5 (50)	4 (36)
Family history of CAD, n (%)	6 (60)	2 (20)	1 (9)
BMI (kg/m ²), mean ± SD	24.51 ± 1.64	27.98 ± 3.86	25.14 ± 2.16
DAC (cm), mean ± SD	84.80 ± 9.53	95.05 ± 10.24	88.95 ± 8.33
Heart rate (bpm), mean ± SD	77.20 ± 14.68	69.40 ± 10.88	70.73 ± 10.70
Systolic BP (mmHg), mean ± SD	123.60 ± 31.28	133.70 ± 21.76	144.45 ± 21.36
Diastolic BP (mmHg), mean ± SD	68.30 ± 24.86	76.70 ± 12.79	81.55 ± 16.31
Laboratory parameters			
TnI (ng/mL), median (IQR 25%–75%)	0.63 (0.02–5.65)	0.19 (0.03–1.05)	0.02 (0.002–0.34)
TnT (ng/mL), median (IQR 25%–75%)	0.65 (0.10–1.53)	0.03 (0.01–0.09)	0.02 (0.01–0.06)
CK (U/L), median (IQR 25%–75%)	277 (77–426)	66 (60–160)	67 (52–97)
CK-MB (ng/mL), median (IQR 25%–75%)	9.75 (4.62–29.28)	2.25 (1.10–4.00)	1.40 (0.80–2.40)
LDH (U/L), median (IQR 25%–75%)	224.50 (170.25–435.50)	189.00 (162.25–218.00)	172.00 (149.00–283.00)
NT-proBNP (pg/mL), median (IQR 25%–75%)	784 (581–914)	256 (123–788)	187 (92–1170)
Scr (μmol/L), mean ± SD	69.41 ± 14.19	68.40 ± 9.20	70.43 ± 16.85
HbA1c (%), median (IQR 25%–75%)	7.08 (6.40–10.48)	7.00 (6.15–8.63)	6.80 (6.20–7.80)
TC (mmol/L), mean ± SD	4.29 ± 0.65	3.74 ± 1.18	3.53 ± 1.06
TG (mmol/L), mean ± SD	1.40 ± 0.50	1.92 ± 0.78	1.23 ± 0.33
HDL (mmol/L), mean ± SD	0.96 ± 0.24	1.13 ± 0.60	1.09 ± 0.30
LDL (mmol/L), mean ± SD	2.56 ± 0.50	1.93 ± 0.84	1.89 ± 0.73
Sodium (mmol/L), mean ± SD	139.67 ± 2.49	141.10 ± 2.05	140.07 ± 2.51
Potassium (mmol/L), mean ± SD	4.08 ± 0.44	3.88 ± 0.32	4.07 ± 0.39
Echocardiography, mean ± SD			
LVEF (%)	58.30 ± 10.19	64.10 ± 3.78	64.55 ± 9.28
E/A	1.12 ± 0.27	0.79 ± 0.15	0.80 ± 0.22
Cardiac index (L/min/m ²)	3.06 ± 0.59	2.74 ± 0.53	2.60 ± 0.53
Concomitant medication, n (%)			
Statin	8 (80)	7 (70)	11 (100)
Aspirin	8 (80)	8 (80)	10 (91)
Clopidogrel/ticagrelor	10 (100)	9 (90)	6 (55)
ACE inhibitor/ARB	5 (50)	4 (40)	3 (27)
Beta blocker	8 (80)	6 (60)	7 (64)
Calcium channel blocker	0 (0)	4 (40)	7 (64)
Insulin	2 (20)	2 (20)	2 (18)

STEMI, ST-segment elevation myocardial infarction; NSTEMI, non-STEMI; UA, unstable angina; PAD, peripheral arterial disease; CAD, coronary atherosclerotic heart disease; BMI, body mass index; BP, blood pressure; TnI, troponin I; IQR, interquartile range; TnT, troponin T; CK, creatine kinase; CK-MB, creatine kinase isoenzyme-MB; LDH, lactate dehydrogenase; NT-proBNP, N-terminal pro-B-type natriuretic peptide; Scr, serum creatinine; HbA1c, hemoglobin A1c; TC, total cholesterol; TG, triacylglycerol; HDL, high-density protein; LDL, low-density protein; LVEF, left-ventricular ejection fraction; E/A, ratio of early to late transmitral flow velocity; ACE, angiotensin-converting enzyme; ARB, angiotensin receptor blocker.

With respect to the comparison between the ACS subgroups, the mean diameter of the initial OA was 1.52 ± 0.40 mm for STEMI, 1.62 ± 0.49 mm for NSTEMI, and 1.62 ± 0.42 mm for UA. The angles between the OA and ICA were 82.33° (77.61° – 86.39°), 69.97° (64.71° – 87.82°), and 71.82° (51.19° – 82.95°) in each of these subgroup, respectively. Similarly, no difference was found in the OA diameter and angle among the ACS subgroups ($P = 0.352$).

Hemodynamic Comparison

Through the blood flow simulation, we obtained streamline charts of each OA model (Figs. 2A, 2B). Every line of the streamline chart showed different colors at different posi-

tions, meaning that the closer it approached the color red, the faster the velocity was at that area. The results of quantitative measurements showed that the median (25th–75th percentile) blood velocities of the initial OA in the HCs were 0.147 m/s (0.099–0.302 m/s) and 0.046 m/s (0.029–0.064 m/s) in patients with ACS. The blood velocity of the initial OA was lower in the ACS group than in the HC group ($P = 0.00007$) (Fig. 2C). In the ACS subgroups, the initial OA blood flow velocities were 0.066 m/s (0.034–0.088 m/s) for STEMI, 0.029 m/s (0.023–0.052 m/s) for NSTEMI, and 0.044 m/s (0.030–0.054 m/s) for UA. Similar differences were found for the blood velocity, which was lower in the STEMI, NSTEMI, and UA groups than in the HC group ($P = 0.008$, $P = 0.001$, and $P = 0.0003$, respectively) (Fig. 2D).

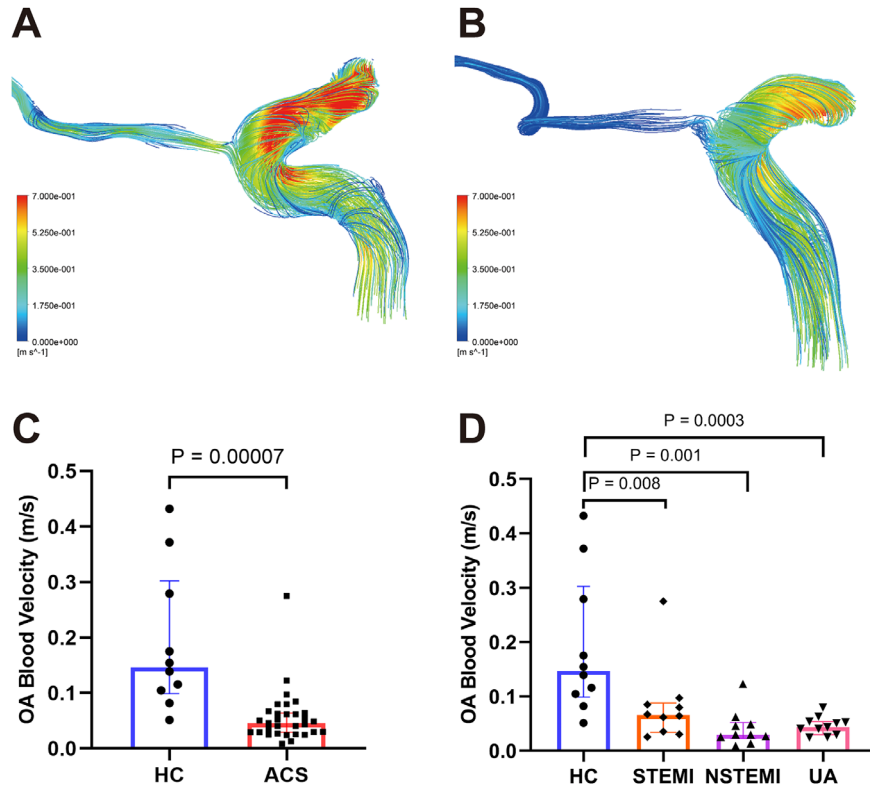


FIGURE 2. The streamlines are colored according to the magnitude of velocity in two typical patients. (A) Streamline of a HC subject. (B) Streamline of an ACS subject; the blood velocity of the OA in the ACS patient was slower than that for the HC. (C, D) Comparisons of OA blood velocities between the ACS and HC groups.

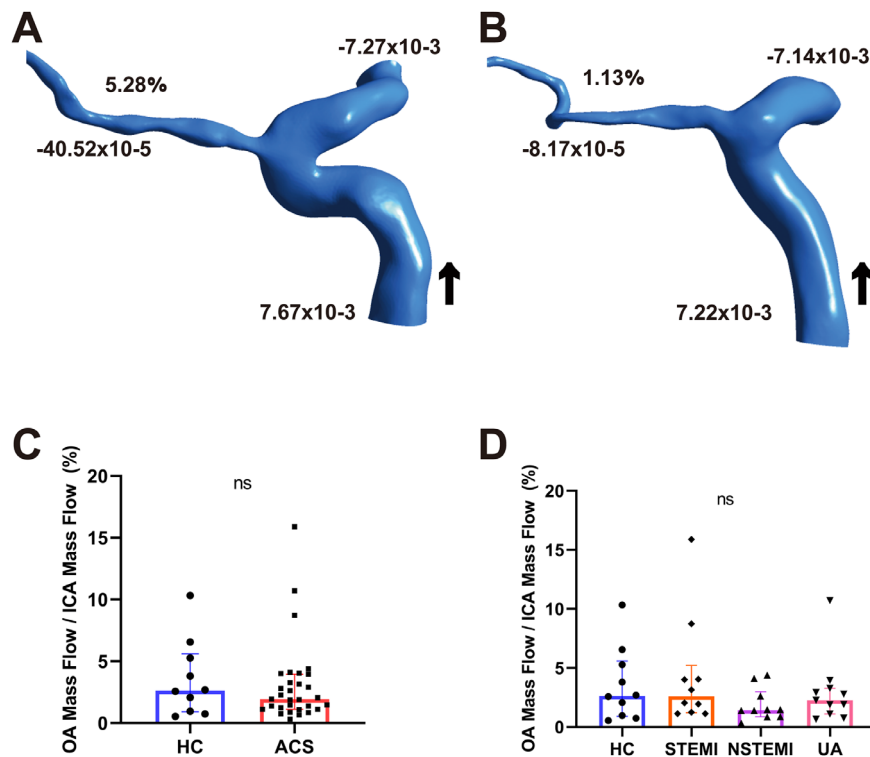


FIGURE 3. Mass flow (kg/s) and mass flow ratio of the OA to ipsilateral ICA (%) of two representative models from HCs (A) and a patient with ACS (B). (C, D) Comparisons of the mass flow ratio of OA to ipsilateral ICA (%) between ACS and HC. Black arrow indicates blood flow direction. ns, not significant; +, inlet; -, outlet.

Figures 3A and 3B show two representative models for mass flow measurements from the HC and ACS groups. The mass flow ratios of OA to ipsilateral ICA were 2.64% (0.91%–5.60%) for the HCs and 1.94% (1.13%–3.95%) for patients with ACS. There was no difference in the mass flow ratio ($P = 0.649$) (Fig. 3C). In the ACS subgroups, the mass flow ratios were 2.60% (1.21%–5.22%) for STEMI, 1.43% (0.87%–2.99%) for NSTEMI, and 2.27% (1.10%–3.28%) for UA. There was no difference in mass flow ratios between the HC and ACS subgroups ($P = 0.497$) (Fig. 3D).

Associations of the OA With ACS Clinical Parameters

Figure 4 displays the correlations of OA blood flow velocity with the clinical parameters of patients with ACS. With regard to clinical characteristics, there was no correlation between blood velocity and age, sex, heart rate, systolic blood pressure, or diastolic blood pressure ($r = 0.320$, $P = 0.079$; $r = -0.157$, $P = 0.400$; $r = 0.029$, $P = 0.877$; $r = -0.035$, $P = 0.853$; and $r = -0.021$, $P = 0.910$, respectively). The OA blood flow velocity was negatively correlated with body mass index (BMI; $r = -0.391$, $P = 0.029$) and abdominal circumference (AC; $r = -0.583$, $P = 0.001$).

With respect to the relationship between echocardiographic parameters and the hemodynamics of the OA, a negative correlation was found between the left ventricular ejection fraction (LVEF) and OA blood flow velocity ($r = -0.412$, $P = 0.021$). In addition, the velocity was positively correlated with the ratio of early to late transmitral flow velocity (E/A; $r = 0.430$, $P = 0.016$), whereas there was no correlation with the cardiac index ($r = -0.008$, $P = 0.965$).

With respect to laboratory parameters related to ACS and prognosis, the OA blood flow velocity was positively correlated with levels of N-terminal pro-B-type natriuretic peptide (NT-proBNP), serum creatinine, and potassium ($r = 0.516$, $P = 0.003$; $r = 0.441$, $P = 0.013$; and $r = 0.377$, $P = 0.036$, respectively) and negatively correlated with triacylglycerol ($r = -0.562$, $P = 0.001$). There were no correlations between OA blood flow velocity and other laboratory markers.

DISCUSSION

We reconstructed 3D models of the OA and simulated blood flow based on CTA, which showed the morphological differences and hemodynamic changes in the OA between patients with ACS and HCs. Because of the small diameter and convoluted course of the OA, it is difficult to clinically observe the initial part of the OA. Previous studies on OA blood flow velocity were conducted using CDI; however, changes in the position of the patient during the examination, the pressure applied by the examiner, and the relative position of the probe could have affected the results.¹⁶ Compared with DSA, CTA is relatively non-invasive, and, compared with CDI, our method displayed the course of the OA more clearly. By measuring the parameters of the OA models, the diameter of the OA at its origin was 1.56 ± 0.37 mm in the HCs, which is different from the results reported by Erdogmus et al. (2.25 ± 0.3 mm on the right and 2.16 ± 0.4 mm on the left).¹⁷ It may be because their study was based on autopsy, and the vascular diameter of cadaver specimens can change after formalin fixation and liquid latex neoprene infusion. Moreover, their study measured the outer diameter of the OA whereas we measured the inner diameter of the OA, which can better reflect the actual state of blood vessels.

Our study showed the blood velocity of the initial OA in patients with ACS was slower than that in HCs. However, retrolubar blood flow data in patients with ACS have not been reported yet. According to available data, the peak systolic and end-diastolic blood velocities of the ophthalmic, central retinal, and short posterior ciliary arteries were reported to be significantly lower in patients with coronary artery disease.¹⁸ This finding is consistent with the results of our study. The basic pathogenesis of ACS is the formation, rupture, and thrombosis of coronary atherosclerotic plaques. Notably, the hemodynamic Doppler pattern in the OA was proposed by many studies to be a predictor of systemic atherosclerosis (AS), including coronary AS.^{19–21} Therefore, we consider the slower blood flow velocity of the OA to be related to AS. It was reported that carotid AS is related to the occurrence and development of coronary AS.²² As the first major branch of the ICA, the OA receives blood from the ICA and can reflect changes in the petrous and cavernous portions of the ICA.²³ Therefore, if the carotid artery devel-

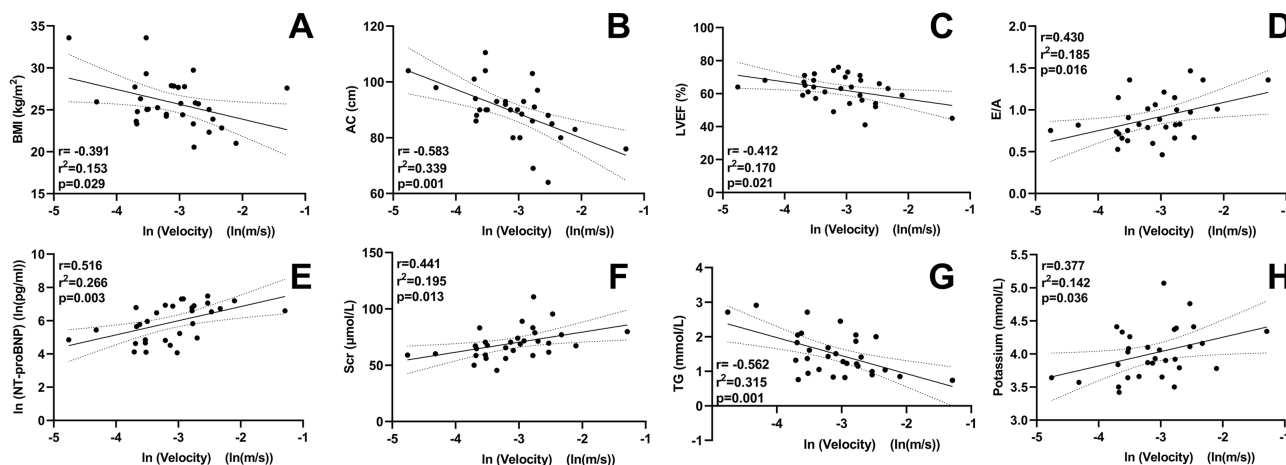


FIGURE 4. Correlation between OA blood velocity and clinical parameters of patients with ACS. Scr, serum creatinine; TG, triacylglycerol; ln, natural log of the variable.

ops AS, the blood velocity will slow down, and the OA will be directly affected, which further confirms our conjecture.

We noted that the E/A and cardiac index of patients with ACS in this study were slightly lower than those of the normal population, which may also be a factor affecting ocular blood velocity. Almeida-Freitas et al.²⁴ found that patients with chronic heart failure had a lower diastolic velocity and a higher resistance index in the OA; thus, the decreased blood flow velocity at the initial stage of OA in patients with ACS may be related to poor cardiac function. In addition, ACS is often accompanied by hypertension, diabetes, hyperlipidemia, and other systemic diseases. The increased resistance or decreased flow in retrobulbar blood flow in patients with hypertension or diabetes have been reported.^{25,26}

Our subgroup study of patients with ACS showed that OA blood velocity in the STEMI group was greater than that in the NSTEMI group. At the same time, the diameter was smaller than that in the NSTEMI group. We believe that this phenomenon is related to compensatory vasoconstriction of the OA in patients with STEMI during CTA. The clinical diagnosis of NSTEMI is not as rapid as that of STEMI, which can be identified based on electrocardiogram (ECG) measurements. The identification of patients with NSTEMI is often delayed due to the frequent lack of clear ECG changes and the uncertainty in the definition of NSTEMI with regard to elevated cardiac troponin levels.²⁷ Therefore, in our study, the smaller vascular diameter and faster blood velocity in the STEMI group than in the NSTEMI group may be related to the timing of the examination. Although the diameter of the OA in the STEMI group was the smallest, there was no statistically significant difference among the groups. This may be related to the small sample size.

The proportion of the OA and ipsilateral ICA blood flow in patients with ACS was smaller than that in HC. However, the difference was not statistically significant. This could be due to a combination of different factors. First, ocular blood flow is autoregulated, and there is a mechanism in the retinal circulation that allows vascular resistance to adapt to changes in perfusion pressure and maintain constant blood flow.²⁸ Second, almost all of our patients underwent PCI or CABG and received well-tolerated drug therapy; this may have resulted in timely improvement of their cardiac function, as observed in the results for the LVEF. Such therapy maintains the pumping function of the heart and ensures blood supply to the carotid artery. Downstream of the ICA, the OA also ensures blood flow. Naturally, there is also the possibility that some patients experienced ocular ischemia; however, this occurrence was not significant due to the small sample size. In addition, if the heart function is damaged for a long time and the carotid artery flow rate continues to be slow, then the OA blood flow may be compensated by dilation.²⁹ There was no statistical difference in OA diameter. The onset of ACS is relatively rapid, and, although we performed CTA only a short time after diagnosis and treatment, the time lapse could have had an effect. In future studies, we will follow up with patients to explore this effect.

In the correlation analysis, clinical indicators were associated with the blood flow velocity of the OA. Among these correlations, BMI and AC were negatively correlated with OA blood flow velocity. Obesity, particularly abdominal obesity, is well known to be associated with increased cardiovascular disease, cancer, and all-cause mortality.³⁰ The average BMI and AC of patients with ACS included in this study

were above the normal values. Hypertriglyceridemia is a major detectable blood abnormality associated with abdominal obesity³¹ that may result from a dual mechanism, including increased secretion of triglyceride-rich lipoproteins and impaired clearance of these lipoproteins.³² This may also explain why triglyceride levels were found to be inversely associated with OA blood flow velocity. From the perspective of biomechanics, slow OA blood flow velocity can increase the residence time for blood to interact with the vessel wall. The longer retention time allows lipids and emboli in the blood to interact with the vessel wall, which can lead to thrombus formation. This provides a new direction for us to analyze the pathogenesis of diseases such as ACS. In addition, we studied many clinical and laboratory indicators closely related to cardiac function. Among these, LVEF was negatively correlated with OA blood flow velocity, and other indicators were positively correlated with it. NT-proBNP is a neurohormone mainly synthesized and secreted by the ventricular myocardium. Although NT-proBNP is commonly used to evaluate patients with heart failure, it is independently associated with the risk of coronary heart disease and poor prognosis in patients with STEMI and NSTEMI.³³ Elevated NT-proBNP levels reflect increased atrial or ventricular stretch due to pressure or volume overload.³⁴ We speculate that there is a regulatory mechanism between OA blood flow and cardiac function that requires further exploration.

This study had some limitations. Because of the cross-sectional design of this study, the variation of the OA overtime was not considered. In future studies, we will follow up with patients to explore this effect. Another limitation is the small sample size. Moreover, the slice thickness and hatch spacing of the CTA scan limited the accuracy of the 3D reconstruction models. Also, almost all of our ACS patients underwent PCI or CABG and received well-tolerated drug therapy, which could have affected the mass flow. Finally, because more research data are not available, we adopted the same boundary conditions in the HC group and the ACS group. We will conduct further research in this area to obtain more accurate results.

CONCLUSIONS

In this first, to our knowledge, systematic study of the morphological and hemodynamic analysis of the OA, a reduction in initial OA blood flow velocity was found in patients with ACS. However, OA morphology and mass flow in patients with ACS did not change significantly. Moreover, the clinical parameters of ACS were related to OA blood flow velocity.

Acknowledgments

The authors thank Anqiang Sun, PhD, and Shuqi Ren, PhD, from Beihang University for their valuable contributions of methods to the study.

Supported by grants from the National Natural Science Foundation of China (81870686), Research Foundation of Beijing Friendship Hospital, Capital Medical University (yyqdkd 2019-29), and Capital's Funds for Health Improvement and Research (2018-1-2021).

Disclosure: **L.-T. Wu**, None; **J.-L. Wang**, None; **Y.-L. Wang**, None

References

- Makki N, Brennan TM, Girotra S. Acute coronary syndrome. *J Intensive Care Med*. 2015;30:186–200.
- Wang J, Zhao M, Li SJ, Wang DZ. Retinal artery lesions and long-term outcome in Chinese patients with acute coronary syndrome. *Eye (Lond)*. 2015;29:643–648.
- Hsien YM, Mustapha M, Hamzah JC, Maskon O, Ken CC, Hamdi CH. Why can't I see after my heart is fixed: a case series of ocular complications after cardiac intervention. *BMC Ophthalmol*. 2016;16:32.
- Woo SC, Lip GY, Lip PL. Associations of retinal artery occlusion and retinal vein occlusion to mortality, stroke, and myocardial infarction: a systematic review. *Eye (Lond)*. 2016;30:1031–1038.
- Chang YS, Chu CC, Weng SF, Chang C, Wang JJ, Jan RL. The risk of acute coronary syndrome after retinal artery occlusion: a population-based cohort study. *Br J Ophthalmol*. 2015;99:227–231.
- Park SJ, Choi NK, Yang BR, et al. Risk and risk periods for stroke and acute myocardial infarction in patients with central retinal artery occlusion. *Ophthalmology*. 2015;122:2336–2343.e2332.
- Werther W, Chu L, Holekamp N, Do DV, Rubio RG. Myocardial infarction and cerebrovascular accident in patients with retinal vein occlusion. *Arch Ophthalmol*. 2011;129:326–331.
- Rim TH, Han JS, Oh J, Kim DW, Kang SM, Chung EJ. Retinal vein occlusion and the risk of acute myocardial infarction development: a 12-year nationwide cohort study. *Sci Rep*. 2016;6:22351.
- Hu CC, Ho JD, Lin HC. Retinal vein occlusion and the risk of acute myocardial infarction (correction of infraction): a 3-year follow-up study. *Br J Ophthalmol*. 2009;93:717–720.
- Arnould L, Guenancia C, Azemar A, et al. The EYE-MI pilot study: a prospective acute coronary syndrome cohort evaluated with retinal optical coherence tomography angiography. *Invest Ophthalmol Vis Sci*. 2018;59:4299–4306.
- Thondapu V, Tenekecioglu E, Poon EKW, et al. Endothelial shear stress 5 years after implantation of a coronary bioresorbable scaffold. *Eur Heart J*. 2018;39:1602–1609.
- Guerciotti B, Vergara C, Azzimonti L, et al. Computational study of the fluid-dynamics in carotids before and after endarterectomy. *J Biomech*. 2016;49:26–38.
- Febina J, Sikkandar MY, Sudharsan NM. Wall shear stress estimation of thoracic aortic aneurysm using computational fluid dynamics. *Comput Math Methods Med*. 2018;2018:7126532.
- Kojima M, Irie K, Fukuda T, Arai F, Hirose Y, Negoro M. The study of flow diversion effects on aneurysm using multiple enterprise stents and two flow diverters. *Asian J Neurosurg*. 2012;7:159–165.
- North American Symptomatic Carotid Endarterectomy Trial Steering Committee. North American Symptomatic Carotid Endarterectomy Trial: methods, patient characteristics, and progress. *Stroke*. 1991;22:711–720.
- Stalmans I, Vandewalle E, Anderson DR, et al. Use of colour Doppler imaging in ocular blood flow research. *Acta Ophthalmol*. 2011;89:e609–e630.
- Erdogmus S, Govsa F. Anatomic features of the intracranial and intracanalicular portions of ophthalmic artery: for the surgical procedures. *Neurosurg Rev*. 2006;29:213–218.
- Krasnicki P, Dmuchowska DA, Proniewska-Skrettek E, Dobrzycki S, Mariak Z. Ocular haemodynamics in patients with type 2 diabetes and coronary artery disease. *Br J Ophthalmol*. 2014;98:675–678.
- Maruyoshi H, Kojima S, Kojima S, et al. Waveform of ophthalmic artery Doppler flow predicts the severity of systemic atherosclerosis. *Circ J*. 2010;74:1251–1256.
- Kojima S, Maruyoshi H, Kojima S, Ogawa H. The waveform index of the ophthalmic artery predicts impaired coronary flow reserve. *Microvasc Res*. 2016;105:30–33.
- Hong SP, Park YW, Lee CW, et al. Usefulness of the Doppler flow of the ophthalmic artery in the evaluation of carotid and coronary atherosclerosis. *Korean Circ J*. 2014;44:406–414.
- Haffner SM, D'Agostino R, Mykkanen L, et al. Proinsulin and insulin concentrations in relation to carotid wall thickness: Insulin Resistance Atherosclerosis Study. *Stroke*. 1998;29:1498–1503.
- Hu HH, Sheng WY, Yen MY, Lai ST, Teng MM. Color Doppler imaging of orbital arteries for detection of carotid occlusive disease. *Stroke*. 1993;24:1196–1203.
- Almeida-Freitas DB, Meira-Freitas D, Melo LA, Jr, Paranhos A, Jr, Iared W, Ajzen S. Color Doppler imaging of the ophthalmic artery in patients with chronic heart failure. *Arq Bras Oftalmol*. 2011;74:326–329.
- Xiao-yong L, Ling L. Clinical significance of postocular artery color Doppler ultrasound in patients with hypertension. *Chin J Front Med Sci*. 2017;9:97–101.
- Divya K, Kanagaraju V, Devanand B, Jeevamala C, Raghuram A, Sundar D. Evaluation of retrobulbar circulation in type 2 diabetic patients using color Doppler imaging. *Indian J Ophthalmol*. 2020;68:1108–1114.
- Ahrens I, Averkov O, Zúñiga EC, et al. Invasive and antiplatelet treatment of patients with non-ST-segment elevation myocardial infarction: understanding and addressing the global risk-treatment paradox. *Clin Cardiol*. 2019;42:1028–1040.
- Delaey C, Van De Voorde J. Regulatory mechanisms in the retinal and choroidal circulation. *Ophthalmic Res*. 2000;32:249–256.
- Luo X, Shen YM, Jiang MN, Lou XF, Shen Y. Ocular blood flow autoregulation mechanisms and methods. *J Ophthalmol*. 2015;2015:864871.
- Hu L, Huang X, You C, et al. Prevalence of overweight, obesity, abdominal obesity and obesity-related risk factors in southern China. *PLoS One*. 2017;12:e0183934.
- Tchernof A, Després JP. Pathophysiology of human visceral obesity: an update. *Physiol Rev*. 2013;93:359–404.
- Björnson E, Adiels M, Taskinen MR, Borén J. Kinetics of plasma triglycerides in abdominal obesity. *Curr Opin Lipidol*. 2017;28:11–18.
- Sterling MR, Durant RW, Bryan J, et al. N-terminal pro-B-type natriuretic peptide and microsize myocardial infarction risk in the reasons for geographic and racial differences in stroke study. *BMC Cardiovasc Disord*. 2018;18:66.
- Linssen GC, Bakker SJ, Voors AA, et al. N-terminal pro-B-type natriuretic peptide is an independent predictor of cardiovascular morbidity and mortality in the general population. *Eur Heart J*. 2010;31:120–127.